Lawrence Berkeley Laboratory
UNIVERSITY OF CALIFORNIA

Invited paper presented at the 5th Adriatic International Conference on Nuclear Physics, Hvar, Yugoslavia, September 24-29, 1984

COMPRESSION AND EXPANSION AT THE BEVALAC

A.M. Poskanzer, K.G.R. Doss, H.-A. Gustafsson, H.H. Gutbrod, B. Kolb, H. Löhner, B. Ludewigt, T. Renner, H. Riedesel, H.G. Ritter, A. Warwick, and H. Wieman

September 1984

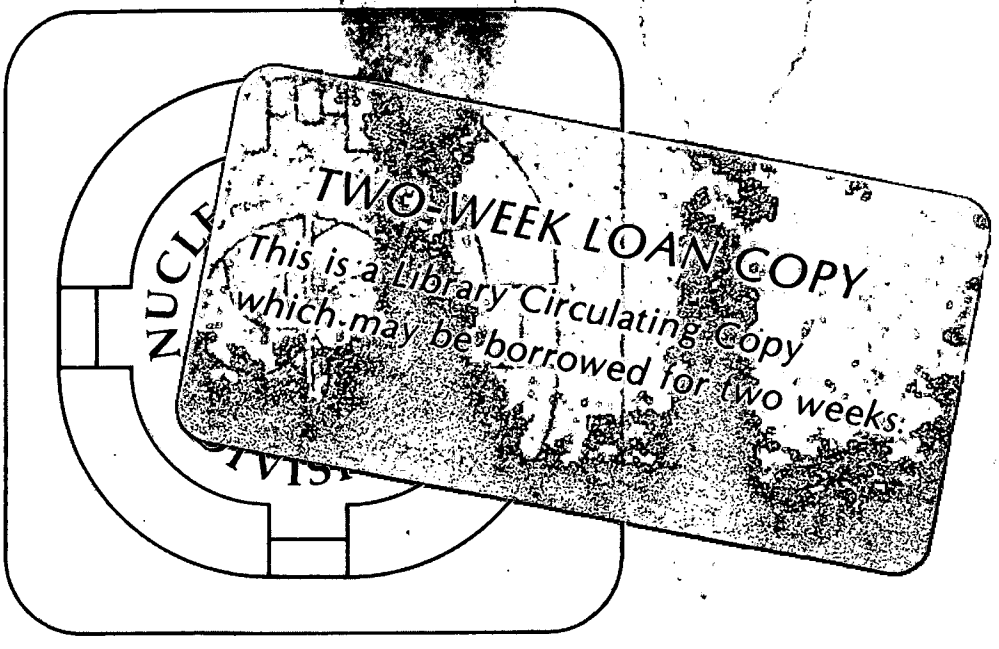

Prepared for the U.S. Department of Energy under Contract DE-AC03-76SF00098

DISCLAIMER

LBL-18357

COMPRESSION AND EXPANSION AT THE BEVALAC*

A. M. Poskanzer, K. G. R. Doss, H.-A. Gustafsson, H. H. Gutbrod, B. Kolb, H. Löhner, B. Ludewigt, T. Renner, H. Riedesel, H. G. Ritter, A. Warwick and H. Wieman

Gesellschaft fur Schwerionenforschung
D-6100 Darmstadt, West Germany

and

Nuclear Science Division
Lawrence Berkeley Laboratory
University of California
Berkeley, CA 94720

Invited paper for the 5th Adriatic International Conference on Nuclear Physics, Hvar, Yugoslavia, 24-29 September 1984

*This work was supported by the Director, Office of Energy Research, Division of Nuclear Physics of the Office of High Energy and Nuclear Physics of the U.S. Department of Energy under Contract DE-AC03-76SF00098.

COMPRESSION AND EXPANSION AT THE BEVALAC*

A. M. Poskanzer, K. G. R. Doss, H.-A. Gustafsson, H. H. Gutbrod, B. Kolb, H. Lohner, B. Ludewigt, T. Renner, H. Riedesel, H. G. Ritter, A. Warwick and H. Wieman

Gesellschaft fur Schwerionenforschung
D-6100 Darmstadt, West Germany

and

Nuclear Science Division
Lawrence Berkeley Laboratory
University of California
Berkeley, CA 94720

ABSTRACT

Recent experimental results from 4π detectors at the Bevalac are presented, with emphasis on the Plastic Ball. Topics discussed are stopping, compression, collective flow, and chemical and thermal freeze-out.

1. OUTLINE

Heavy nuclei, in central collisions at Bevalac energies, stop in their center of mass producing a region of equilibrated, hot matter. Some of the energy is stored as potential energy of compression. At the same time the pressure builds up, producing a sidewise collective flow of nuclear matter. The system then expands until the density is reduced so that the chemical equilibria producing the light composite nuclei freeze-out, and then even further until the thermal two body interactions freeze-out. Each of these points will be documented.

2. PLASTIC BALL[1]

The Plastic Ball covers the angular region between 10 and 160

*This work was supported by the Director, Office of Energy Research, Division of Nuclear Physics of the Office of High Energy and Nuclear Physics of the U.S. Department of Energy under Contract DE-AC03-76SF00098.

deg. It consists of 815 detectors where each module is a ΔE-E telescope capable of identifying the hydrogen and helium isotopes and positive pions. The ΔE measurement is performed with a 4-mm thick CaF_2 crystal and the E counter is a 36-cm long plastic scintillator. Both signals are read out by a single photomultiplier tube. Due to the different decay times of the two scintillators, ΔE and E information can be separated by gating two different ADCs at different times. The positive pions are additionally identified by measuring their delayed decay.

The Plastic Wall, placed 6 m downstream from the target, covers the angular range from 0 to 10 deg. and measures time of flight, energy loss and position of the reaction proucts. In addition, the information from the inner counters (0 to 2 deg.) is used to produce a trigger signal.

3. STOPPING

By measuring in each event the momentum distribution of the fragments in the center of mass system the degree of thermalization can be determined. For an isotropically expanding system one finds in the center-of-mass frame from simple phase space considerations:

$$\frac{2}{\pi} \sum_i |p_\perp^i| = \sum_i |p_\parallel^i| \quad . \tag{1}$$

The sums in eq. (1) contain the perpendicular, $p_\perp$, and longitudinal, $p_\parallel$, momentum components of all particles in an event. A global stopping of the two nuclei in the center of mass system would show up by the two sides of eq. (1) being equal, or $p_\perp$ even larger if flow into the transverse direction exists. In the presence of transparency $p_\parallel$ would always be larger. Isotropy is a necessary but not sufficient condition for thermalization. If in addition the energy distributions are of Maxwell-Boltzmann type the emitting system may be called thermalized.

Plastic Ball data[2] are shown in Fig. 1. In Fig. 1 (top) contour lines of the event yield accumulated with the minimimum bias trigger

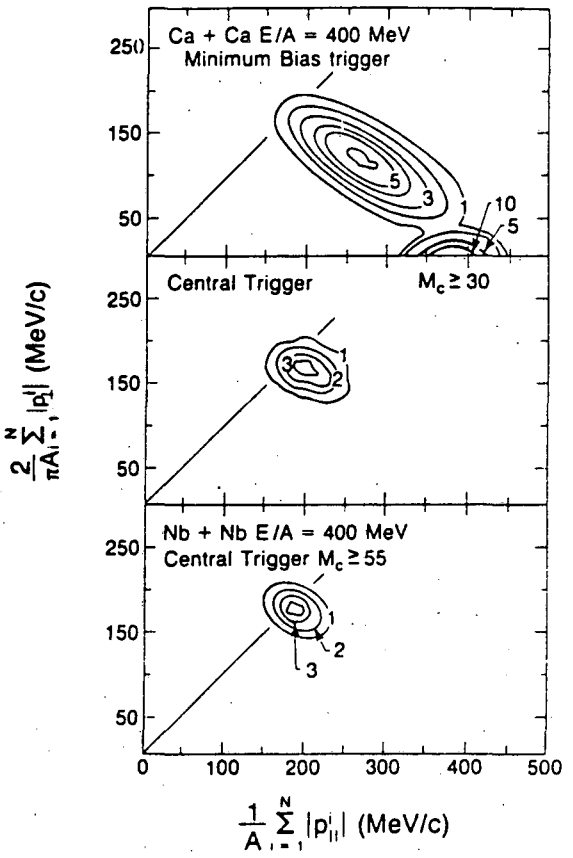

Fig. 1. Contour plots of the average particle momentum components perpendicular and parallel to the beam axis for Ca + Ca (top and center) and Nb + Nb (bottom) at E/A = 400 MeV. The diagonal line corresponds to isotropic events.

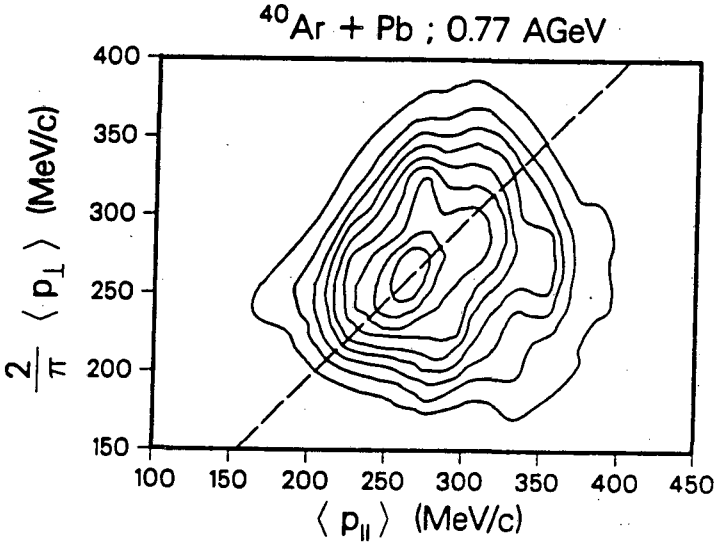

Fig. 2. Contour plot of average perpendicular and parallel momentum for 770 MeV/A ^{40}Ar on Pb with a high multiplicity cut.[3]

are shown in the $p_\perp$ versus $p_\parallel$ plane for the Ca + Ca system. The peak at small $p_\perp$ but large $p_\parallel$ corresponds to peripheral reactions and is dominated by projectile fragments. This contribution vanishes as the trigger is changed to a "central" one. Fig. 1 (center) shows central trigger events with a charged particle multiplicity larger than 30. The maximum of the yield is shifted towards the diagonal but only a few events reach it, which corresponds to full stopping of the nuclei. In the lower part of fig. 1 for the reaction of 400 MeV/nucleon Nb + Nb the central trigger events with charged particle multiplicities M_c larger than 55 almost fulfill the stopping and isotropy condition on the average.

Fig. 2 shows the same kind of plot from the Streamer Chamber[3] for 770 MeV/A ^{40}Ar on Pb with a high multiplicity cut. For this central collision of a medium weight projectile on a heavy target there is complete diving at the projectile into the target, again leading to stopping in the center of mass of the participants.

4. COMPRESSION

"An estimate of the energy tied up in compression at the maximum-density phase of the collision has been given by Stock et al.[4,5] They used the streamer chamber to study ^{40}Ar + KCl as a function of energy. At each energy the π^- yield was measured as a function of proton partcipant number and extrapolated to b = 0, as shown in fig. 3. The results shown in fig. 4 indicate as a function of energy a substantial reduction below predictions either of cascade calculations or of a chemical model, though the theories agree with each other. The interpretation offered is simple: at each beam energy, if the energy available for pion production is reduced by the amount shown by the horizontal arrows in fig. 4 the correct number of pions would be obtained. The deficiency is attributed to energy required to compress the nuclear matter, which is not allowed for in the theoretical results. Since the theories provide the density reached in the collision it is possible to go one step further and derive an equation of state for nuclear matter, as shown in fig. 5. Despite criticism of

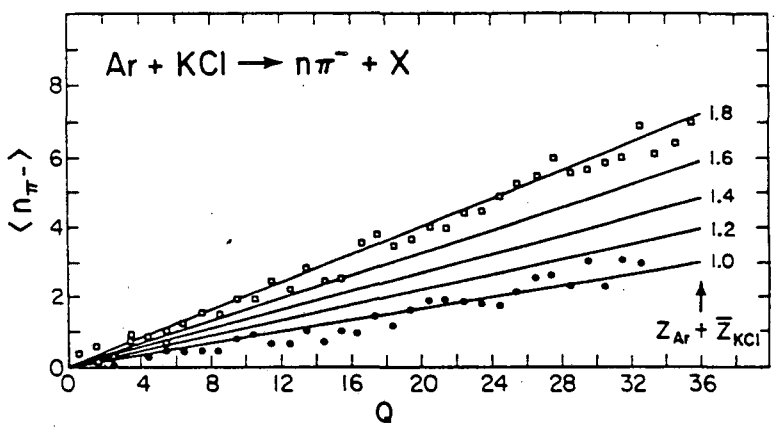

Fig. 3. The mean π^--multiplicity observed[5] in Ar + KCl reactions at 1.0, 1.2, 1.4, 1.6 and 1.8 GeV/u plotted as a function of the observed number of proton participants Q. Only the interpolating lines are shown except for 1.0 and 1.8 GeV/u.

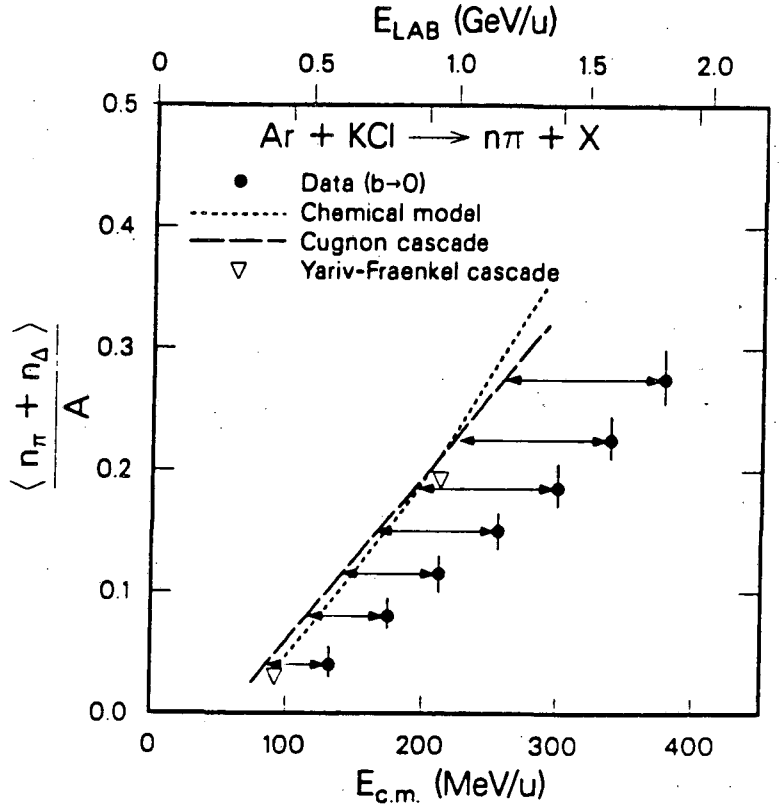

Fig. 4. The π + Δ yield per participant nucleon is plotted as a function of c.m. energy (lower axis) and laboratory energy (upper axis) for Ar + KCl.[5] The solid circles are the experimental results for zero impact parameter. The dashed and dotted curves correspond to the Cugnon cascade and the chemical model predictions, respectively, and the triangles are predictions of the Yariv-Fraenkel cascade. The horizontal arrows represent the values of the compressional energy per nucleon E_c determined at each experimental point.

the procedure in detail, the concept has not been invalidated and it remains as the only means so far of extracting an equation of state from experimental data."[6]

5. COLLECTIVE FLOW

Direct evidence of the compression effects predicted by an equation of state would be collective flow of the nuclear matter upon re-expansion. Data from 4π detectors like the Plastic Ball are ideally suited for studying the emission patterns and event shapes which might be able to reveal this effect and distinguish between predictions of cascade and hydrodynamical models.

The sphericity tensor

$$F_{ij} = \sum_{\nu} p_i(\nu)p_j(\nu)w(\nu) \qquad (2)$$

is calculated from the momenta of all measured particles for each event. It is appropriate to choose the weight factor $w(\nu)$ in such a way that composite particles have the same weight per nucleon as the individual nucleons of the composite particle at the same velocity. For the Plastic Ball analyses the weight $w(\nu) = 1/2m(\nu)$ (kinetic energy flow) is used. Another coalescence-invariant weight $1/p(\nu)$ has been used in the analysis of the Streamer Chamber results to be shown.

The sphericity tensor approximates the event shape by an ellipsoid whose orientation in space and whose aspect ratios can be calculated by diagonalization. The shapes predicted by hydrodynamical and intranuclear cascade calculations are quite different. The hydrodynamical model predicts prolate shapes along the beam axis only for grazing collisions but with decreasing impact parameter the flow angle increases, and reaches 90 deg. (with oblate shapes) for zero-impact-parameter events. Simple cascade calculations on the other hand predict zero flow angles at all impact parameters.

Approximately 50,000 Plastic Ball events accumulated with a minimum-bias trigger have been analyzed for both Ca and Nb collisions.[7] The distribution of the flow angle θ (angle between the

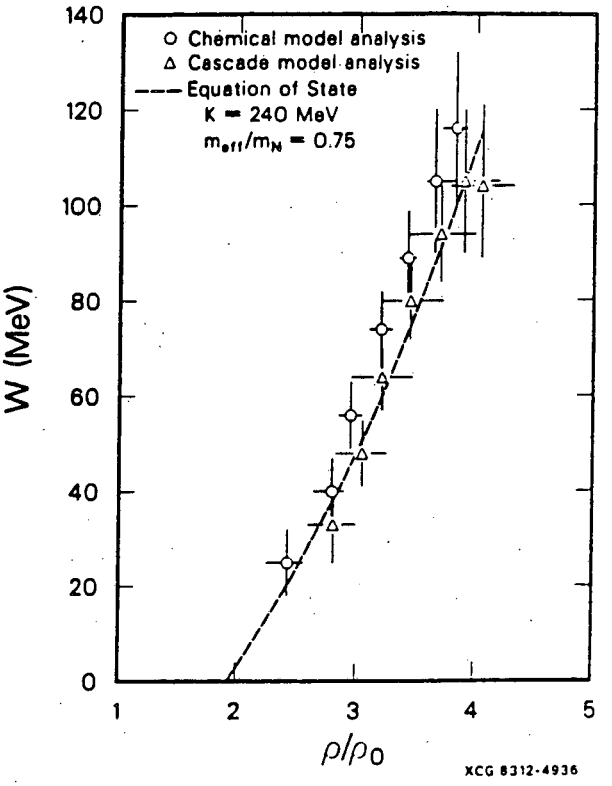

Fig. 5. Values of the compressional energy, minus 10 MeV binding energy, plotted as a function of the density in units of normal nuclear density ρ_0 derived from the data using the cascade and chemical model, respectively.[5] Only statistical errors are given. The curve is a relativistic field theoretical prediction with K = 240 MeV and m_{eff} = 0.75 m_N.

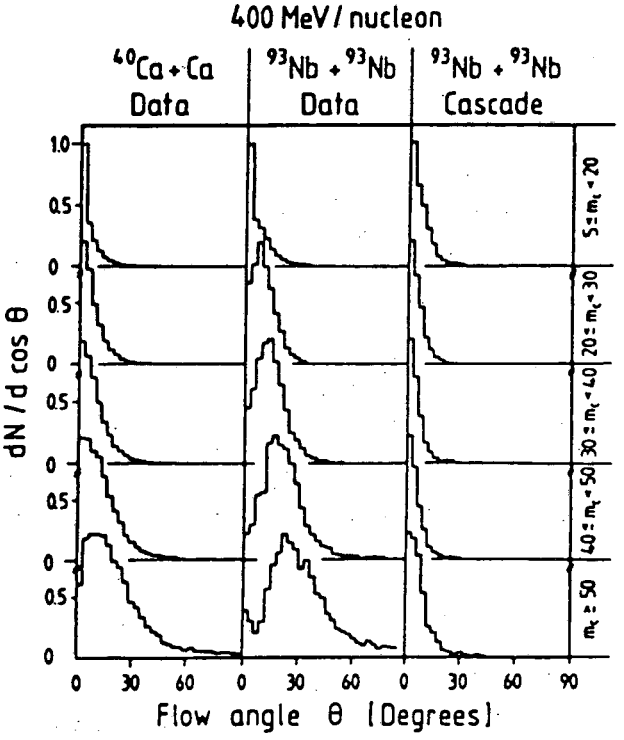

Fig. 6. Frequency distributions of the flow angle θ for two sets of data and a cascade calculation for different multiplicity bins. For the case of Ca the multiplicities are half the indicated values.

major axis of the flow ellipsoid and the beam axis) is shown in fig. 6 for different multiplicity selections. A striking difference between the Ca and Nb data can be observed. For all but the highest multiplicity bins the distribution of the flow angles for the Ca data is peaked at 0 deg. For Nb, however, there is a finite deflection angle increasing with increasing multiplicity. The same analysis has been performed with filtered events from a cascade code calculation (fig. 6). For both systems studied the distributions are always peaked at 0 deg. It is not so evident that the Ca + Ca collision differs from its simulation with the cascade model, whereas a new collective phenomenon definitely appears in the larger-mass system which is not accounted for by the present cascade models.

In this analysis each event was parametrized by an ellipsoid, but it is of interest to study the shapes in more detail. The fact that finite flow angles are seen in the data indicates that in those events a reaction plane exists that is defined by the flow axis and the beam axis. All events can be rotated by the azimuthal angle ϕ determined by the flow analysis so that their individual reaction planes all fall into the x-z plane, with the z axis being the beam axis. For those rotated events the invariant cross section in the reaction plane $[d^2\sigma/dy\ d(p_x/m)]$ can be plotted, where p_x is the projection of the perpendicular momentum into the reaction plane and y is the center-of-mass rapidity. In addition, because of detector inefficiency near the target rapidity, the graphs in fig. 7 have been reflected about 90 deg. in the center of mass for didactic reasons.

The highest level contour, near projectile rapidity and just above the horizontal axis, results largely from the projectile remnants and indicates a definite bounceoff effect. The bounceoff process is a slowing down of the projectile fragments and a sidewards deflection in the reaction plane. The data show that the multiplicity dependence of the orientation of the outer contour lines from the lower left to the upper right follows the trend indicated by the flow-angle distributions (fig. 6). However, the position of the bounceoff peak from the projectile remnants changes only slightly with multiplicity. Thus one can conclude that the strong sideward peaking seen in fig. 6, which we

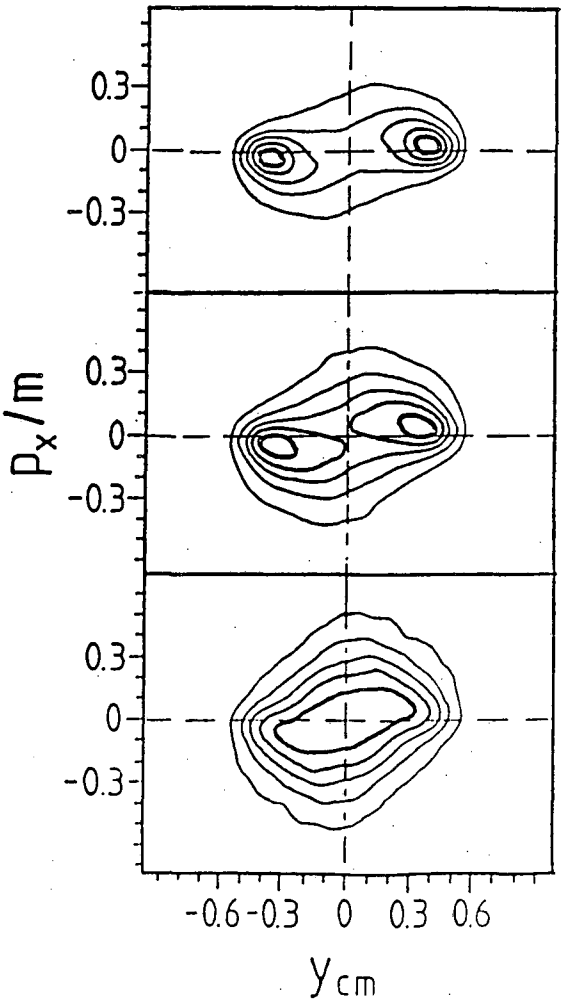

Fig. 7. Contour plots (equally-spaced linear contours without offset) of P_x/m as a function of c.m. rapidity for multiplicities of 30-39, 40-49, and greater than 50.

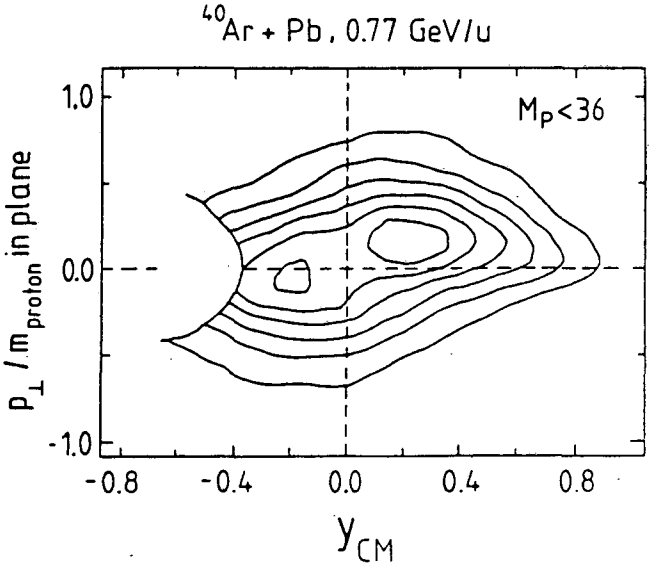

Fig. 8. Contour plot of data after rotation of each event to make all the reaction planes coincide.[3] The quantity $p_\perp/m$ is plotted vs. $y_{c.m.}$ From the multiplicity selection the impact parameters are thought to be $3.0 < b < 5.5$ fm.

will call side splash, is mainly due to the midrapidity particles. It should be noted that the bounceoff and side-splash effects appear to be in the same plane.

The hydrodynamical prediction of the flow angle seems to be qualitatively in agreement with the measurement, but the present models do not predict two separate effects as seen in the data.

Streamer Chamber data for an asymmetric system is shown plotted the same way in fig. 8. It is for low M_p, 3 fm < b < 5.5 fm (the cut shows the region of detector inefficiency near the target). The graph shows an average sideways deflection of the participants. However, for this asymmetric system the events become spherical at high multiplicity corresponding to complete diving of the projectile into the target.

6. CHEMICAL FREEZE-OUT[8]

One of the major goals in the study of composite particle production is to extract information about the size and density of the participant volume. The d/p ratio determines the volume of the system at freeze-out. To determine the density one needs the number of baryons in this volume. We define N_p as the participant baryon charge multiplicity. It also counts those participant protons bound in clusters (d, t, ^{3}He, ^{4}He). These contribute up to about 40% to N_p. Since only the participant multiplicity is wanted, cuts are applied to eliminate the contribution from the spectators. The participant baryon charge multiplicity, N_p, will be abbreviated to proton multiplicity.

The definition of d_{like} is given by

$$d_{like} = d + 3/2(t + {}^3He) + 3({}^4He) \tag{3}$$

and the quantity p_{like} is defined as

$$p_{like} = p + d + t + 2({}^3He + {}^4He) \quad . \tag{4}$$

The functional form of the observed d_{like}/p_{like} ratios can be un-

derstood in terms of the coalescence model. We have used an improved version of the model which is a complete 6 dimensional phase space calculation relating the radii of the deuteron and the particpant zone to the coordinate space, and the temperature of the interacting region to the momentum space. In this model the radius r_p and the temperature T of the interacting region as well as the deuteron radius r_d are related to d_{like} and p_{like} through

$$d_{like}/p_{like} = 6((A - Z)/Z)(1 + 2(r_p/r_d)^2)^{-3/2}N_p \times (1 + 2mTr_d^2/3)^{-3/2} \quad (5)$$

where the factor for (A - Z)/Z makes up for the difference between neutron and proton number and m is the nucleon mass. The radius r_p assuming a spherical source is parametrized as $r_p = r_o((A/Z)N_p)^{1/3}$, where A/Z is the factor converting the participant baryon charge multiplicity to participant baryon multiplicity. The reduced radius, r_o, is then related to the density by $\rho = 1/(4\pi r_o^3/3)$.

In the fits to the observed ratios, r_o and r_d were free parameters. The temperature T was taken to be the mean temperature obtained from Boltzmann fits[2] to the proton spectra at 90 deg. in the center-of-mass system. The fits to the experimental ratios were done for $N_p > 5$ and the results are presented as solid curves in fig. 9. The r_o values are the rms values for a Gaussian density distribution. To convert these values to equivalent sharp sphere radii the values have to be multiplied by $\sqrt{5/3}$. The mean sharp sphere r_o values obtained from the four cases studied correspond to freeze-out densities of 50 to 100% times normal nuclear density.

7. THERMAL FREEZE-OUT DENSITY[9]

Proton-proton correlations were measured with the Plastic Ball which has several features that are of significant value in this application: a large solid angle and rapid data-collection ability, and the ability to detect most of the charged particles in each event,

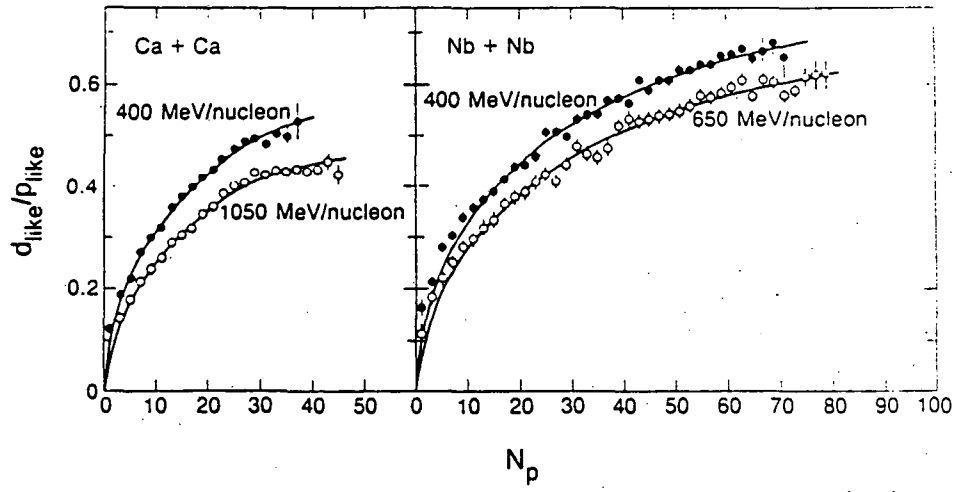

Fig. 9. d_{like}/p_{like} as a function of proton multiplicity (N_p) for the two systems Ca + Ca at 400 and 1050 MeV/nucleon and Nb + Nb at 400 and 650 MeV/nucleon. The curves shown are from fits to eq. (5).

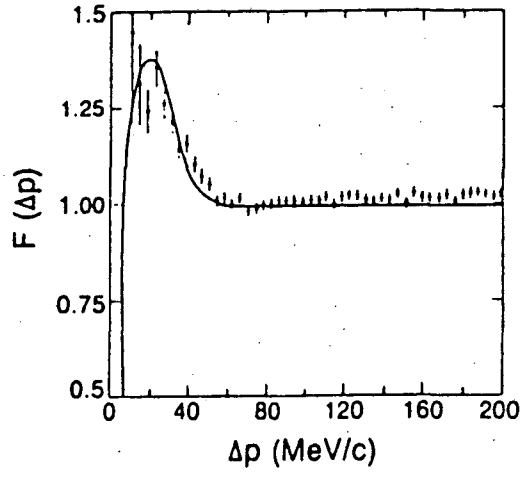

Fig. 10. The measured proton-proton correlation function for Ca + Ca with a proton multiplicity from 25 to 32. The solid curve is a least-squares fit interpolation between distorted theoretical correlation functions for radii of 4 and 5 fm which differ from each other by 25% at the peak.

thus obtaining a direct measure of the participant multiplicity which is necessary for the determination of the freeze-out density. The main difficulty, that the resolution is limited by the finite angular size of the detector modules, has been overcome by smearing the theoretical calculation, thus permitting a direct comparison with the measurement.

Proton-proton correlations came into use for source-size measurements followng the correlation predictions of Koonin which, in addition to the second-order interference effect due to quantum statistics, also include nuclear and Coulomb-induced final-state interactions between the two outgoing protons. At $\Delta p = 0$ the correlation function is zero as a result of the Coulomb repulsion. A peak in the correlation function at $\Delta p = 20$ MeV/c is generated by the attractive nuclear force. The amplitude of this enhanced correlation is strongly dependent on the source-size parameter r_g and increases as the source gets smaller. The degree of correlation between the two protons is strongest when they are close in space, time, momentum. In the general form of Koonin's calculation the proton source density is treated as isotropic with a Gaussian distribution in space and time, and the proton momenta are assumed to be independent of position. The Gaussian spatial density, $p(r) = \exp[(-r/r_g)^2]$, may be thought of as representing the proton positions at the point of their last scattering. For our analysis we assume that the time parameter is zero, i.e., all the protons are emitted at the same time.

Radii have been extracted by comparing measured correlation functions to theoretical predictions which depend on the source-size radius. In practice, the correlation function is obtained from the data as a function of Δp (either one of the proton momenta transformed into the center of mass of the pair) by summing all p-p pairs, event by event, in bins $[N_{true}(\Delta p)]$ according to Δp, and dividing by p-p pairs from different events $[N_{mixed}(\Delta p)]$ to give

$$F(\Delta p) = \text{norm} \times N_{true}(\Delta p)/N_{mixed}(\Delta p) \quad . \tag{6}$$

In forming the mixed-pair sums each proton was paired with each proton

in the preceding five events so that the statistical error in the ratio due to the mixed-event pairs could be neglected compared to the true-pair statistics. It should be pointed out that the Plastic Ball has a reduced efficiency for detecting pairs in the low-Δp region since these pairs will tend to go both into the same detector. However, the correlation function is well determined at Δp = 20 MeV and above and thus gives a good measure of the radius. In fig. 10 we show an example of a measured correlation function along with the distorted theoretical correlation function.

The extracted radii are shown as a function of proton multiplicity in fig. 11. The error bars represent statistical errors only. For both the Ca + Ca and Nb + Nb systems the radius increases with multiplicity. The radii are shown with a fit using the function $r_g = r_o(N_p A/Z)^{1/3}/(\frac{5}{2})^{1/2}$ where r_o is a reduced radius (inversely proportional to the density). N_p is the participant baryon charge multiplicity and A/Z has been included to reflect the presence of neutrons. The extracted radii are the radius parameters for a Gaussian source distribution, and so by inclusion of $(\frac{5}{2})^{1/2}$ in the above function r_o becomes the radius parameter of an rms-equivalent sharp sphere. The value of r_o extracted from the fits is 1.9 fm for the two systems studied. Comparing this directly with r_o = 1.2 fm, the sharp-sphere r_o for normal nuclei, yields a participant-region thermal freeze-out density about 25% of normal nuclear density.

8. ACKNOWLEDGEMENTS

We would like to thank the GSI-LBL Streamer Chamber group, in particular Howel Pugh, for supplying material.

This work was supported by the Director, Office of Energy Research, Division of Nuclear Physics of the Office of High Energy and Nuclear Physics of the U.S. Department of Energy under Contract DE-AC03-76SF00098.

9. REFERENCES

1. Baden, A., Gutbrod, H.H., Löhner, H., Maier, M.R., Poskanzer,

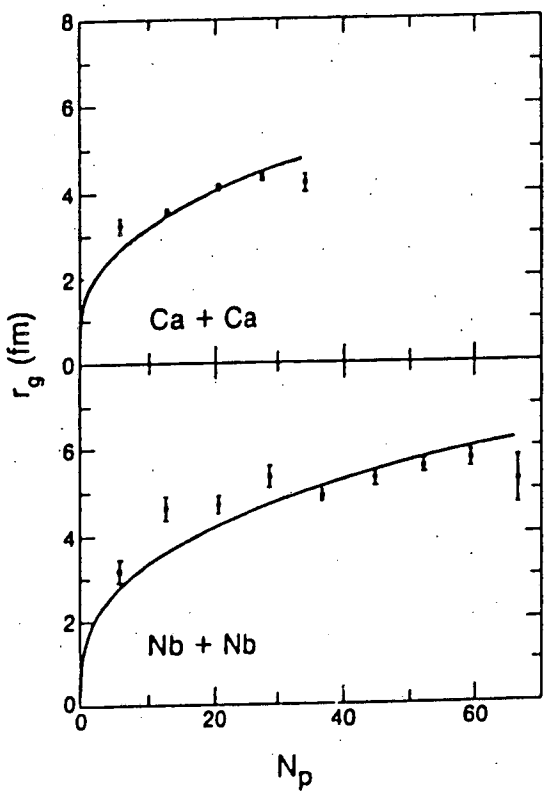

Fig. 11. Extracted Gaussian source radii as a function of proton multiplicity (N_p) for the two systems Ca + Ca and Nb + Nb at 400 MeV/nucleon. The curves are fits to the results with the function $r_g = r_o(N_p A/Z)^{1/3}/(\frac{5}{2})^{1/2}$.

A.M., Renner, T., Riedesel, H., Ritter, H.G., Spieler, H., Warwick, A., Weik, F. and Wieman, H., "The Plastic Ball Spectrometer: An Electronic 4π Detector with Particle Identification", Nucl. Instr. and Meth. 203, 189-211 (1982).

2. Gustafsson, H.-A., Gutbrod, H.H., Kolb, B., Löhner, H., Ludewigt, B., Poskanzer, A.M., Renner, T., Riedesel, H., Ritter, H., Warwick, A. and Wieman, H., "Thermalization in High Energy Nuclear Collisions", Phys. Lett. 142B, 141 (1984).

3. Renfordt, R.E., Schall, D., Bock, R., Brockmann, R., Harris, J.W., Sandoval, A., Stock, R., Ströbele, H., Bangert, D., Rauch, W., Odyniec, G., Pugh, H.G. and Schroeder, L.S., "Stopping Power and Collective Flow of Nuclear Matter in the Reaction Ar + Pb at 0.8 GeV/u", Phys. Rev. Lett. 53, 763 (1984).

4. Stock, R., Bock, R., Brockmann, R., Harris, J.W., Sandoval, A., Ströbele, H., Wolf, K.L., Pugh, H.G., Schroeder, L.S., Maier, M., Renfordt, R., Dacal, A. and Ortiz, M.E., "Compression Effects in Relativistic Nucleus-Nucleus Collisions", Phys. Rev. Lett. 49., 1236 (1982).

5. Harris, J.W., Stock, R., Bock, R., Brockmann, R., Sandoval, A., Ströbele, H., Odyniec, G., Pugh, H.G., Schroeder, L.S., Renfordt, R.E., Schall, D., Bangert, D., Rauch, W. and Wolf, K.L., "Pion Production as a Probe of the Nuclear Matter Equation of State", submitted to Phys. Rev. C (1984).

6. Pugh, H.G., Proceedings of the Fourth International Conference on Ultrarelativistic Nucleus-Nucleus Collisions, Helsinki, June 1984.

7. Gustafsson, H.-A., Gutbrod, H.H., Kolb, B., Löhner, H., Ludewigt, B., Poskanzer, A.M., Renner, T., Riedesel, H., Ritter, H., Warwick, A., Weik, F. and Wieman, H., "Collective Flow Observed in Relativistic Nuclear Collisions", Phys. Rev. Lett. 52, 1590 (1984).

8. Doss, K.G.R., Gustafsson, H.-A., Gutbrod, H.H., Kolb, B., Löhner, H., Ludewigt, B., Poskanzer, A.M., Renner, T., Riedesel, H., Ritter, H.G., Warwick, A. and Wieman, H., "Composite Particles and Entropy Production in Relativistic Nuclear Collisions", to be submitted to Phys. Rev. C.

9. Gustafsson, H.-A., Gutbrod, H.H., Kolb, B., Löhner, H., Ludewigt, B., Poskanzer, A.M., Renner, T., Riedesel, H., Ritter, H., Warwick, A., Weik, F. and Wieman, H., "Freezeout Density in Relativistic Nuclear Collisions Measured by Proton-Proton Correlations", Phys. Rev. Lett. 53, 544 (1984).

TECHNICAL INFORMATION DEPARTMENT
LAWRENCE BERKELEY LABORATORY
UNIVERSITY OF CALIFORNIA
BERKELEY, CALIFORNIA 94720